Development of Quantitative Structure-Activity Relationship for Prediction of Biological Effects of Nanoparticles Associated with Semiconductor Industries (*Task Number: 425.025*)

PIs:

- **Yongsheng Chen, Environmental Engineering, Georgia Institute of Technology (GIT)**

Graduate Students:

- **Wen Zhang: PhD student, Environmental Engineering, GIT**
- **Steven Klein: PhD student, Mechanical engineering, ASU**

Other Researchers:

- **Trevor J. Thornton, Electric Engineering, ASU**
- **Jonathan Posner, Mechanical Engineering, ASU**

Cost Share (other than core ERC funding):

- **$25 k start-up fund from ASU**
- **$152k funds from GIT for AFM and other lab instrument purchase**

Objectives

Develop a quantitative structure-activity relationships (QSARs) model for prediction of the biological effects of engineered nanoparticles (NPs) associated with semiconductor industries. To pursue this goal, our approach mainly includes:

- **Development of new surrogate descriptors (relative to those for conventional contaminants) for NPs and Methodology development of experimental measurement.**
- **Correlation of the descriptors with their environmental behaviors and impact.**

ESH Metrics and Impact

1. *Our work aims at new descriptor development for cytotoxicity of NPs to human health and provides a comprehensive understanding and clear definition of ESH-problematic manufactured nanomaterials.*

2. *Based on the quantitative structure-activity relationship (QSAR) model we plan to establish, problematic nanomateirals from industrial manufacturers could be identified and effectively reduced, and more environmental benign nanomaterials can be designed.*

Bias of traditional descriptors for NPs: study of octanol-water partitioning coefficients (Kow)

A

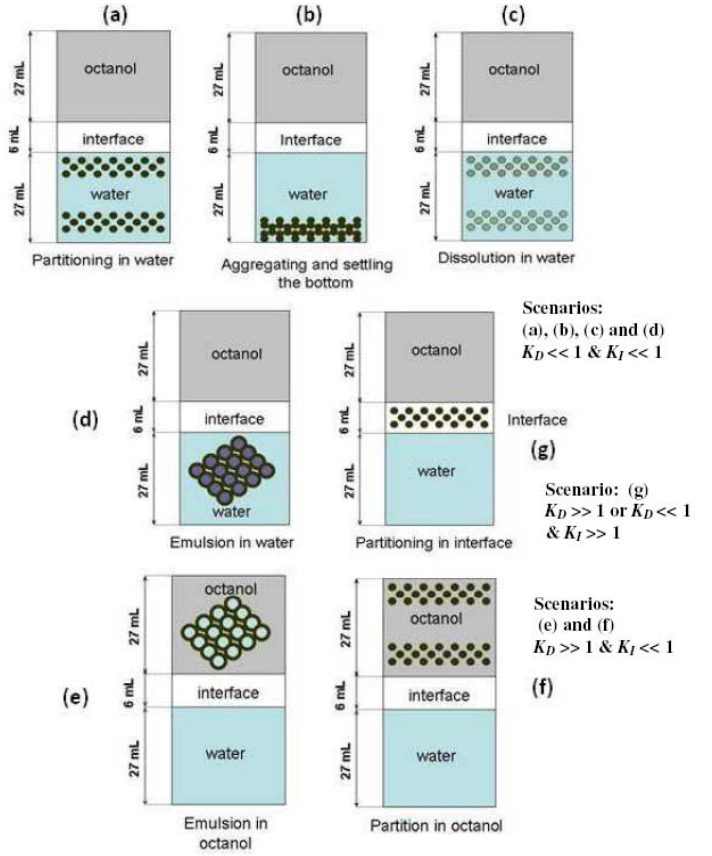

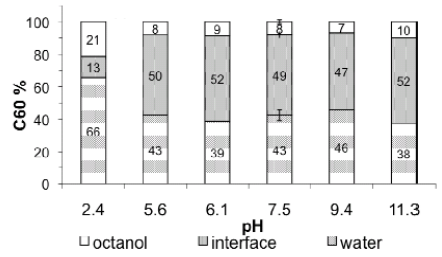

B

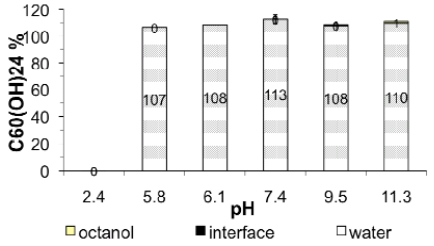

C

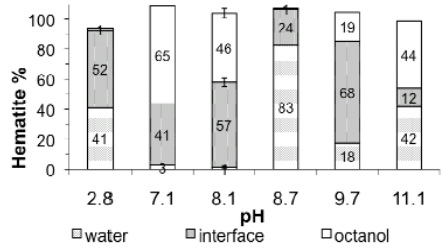

D

Findings: NPs display complex partitioning scenarios (into the octanol phase, water phase, and interface), and pH/ionic strength/presence of natural organic matter all can alter the partitioning state due to uncontrollable mechanisms (e.g., aggregation/dissociation leads to size differences under a wide range of pH or ionic strengths).

A: Boundary partitioning scenarios (a~g) of nanoparticles in the octanol and aqueous phases and the interface. B: Partitioning of n-C_{60}, C: n-$C_{60}(OH)_{24}$ D: hematite nanoparticles in the interface, octanol, and aqueous phases at different pH values in the presence of 1 mM $NaHCO_3$ buffer.

Method and materials: New descriptor development
1. Adhesion force measurement with AFM

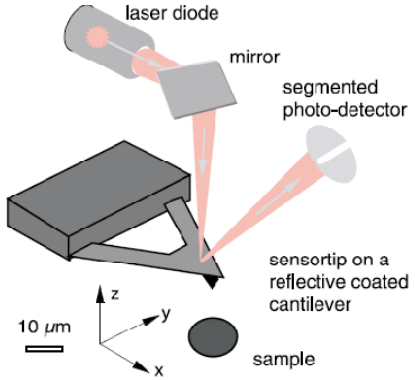

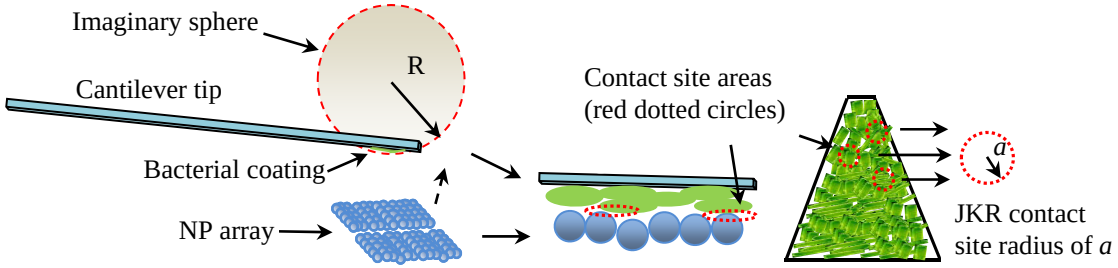

Demonstrations of adhesion force measurement with AFM and determination of contact area with JKR model. Cantilever probe coated with bacterial cells is approaching to NP array and the contact surface of the probe is assumed to be a part of the surface on the imaginary sphere (*R*). Multiple contact sites (indicated by the red circles) between bacteria and NPs add up to a total contact site area of πa^2.

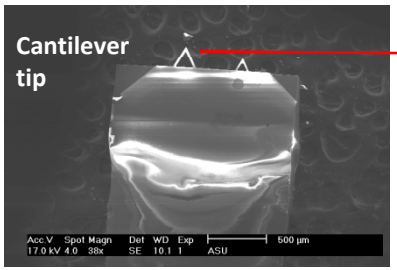

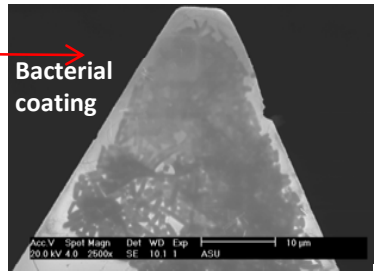

Coating process with micromanipulator

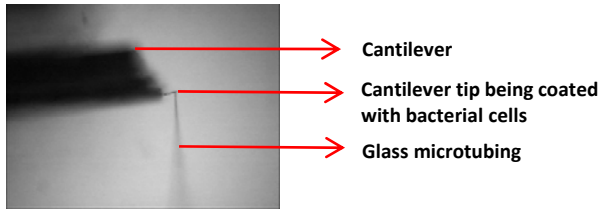

Images of NP array achieved by tapping mode AFM:

NP array composed of NPs (different sizes were determined by Malvern Zetasizer)

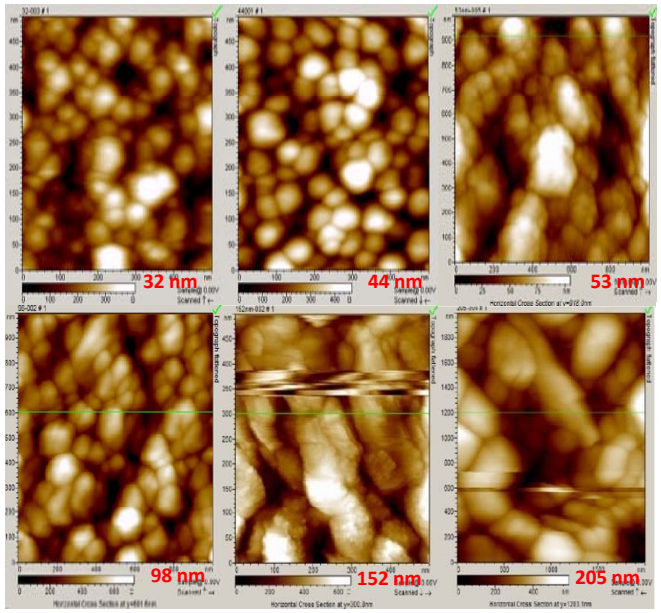

Results and discussion: 1.1 Size effect on Adhesion force between E. coli cells and hematite NPs

Representative interaction force-distance curves for different sizes of NP array probed by *E. coli* cells. (a) 26 nm. (b) 44 nm. (c) 53 nm. (d) 98 nm. (e) 152 nm. (f) Average adhesion force for different sizes of NPs (horizontal error bars indicate standard deviation of particle diameter and vertical error bars indicate standard deviation of adhesion force). n is the number of force measurements for each sample.

Significance: Adhesion forces between *E. coli* cells and hematite NPs decreased as particle size increased as Figure 3 showed and our model of the effective contact area fitted the trend.

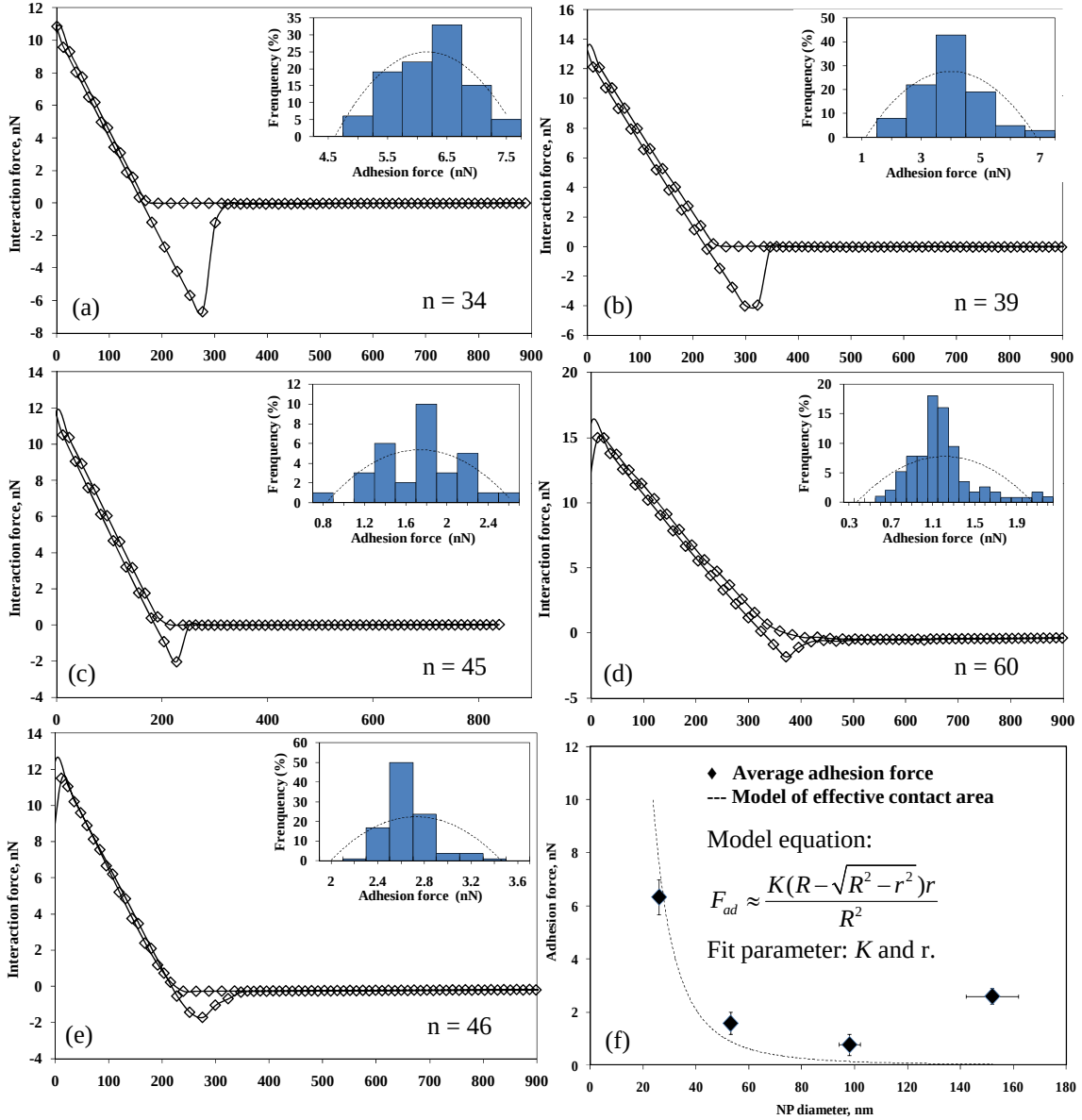

Results and discussion:
1.2 Modeling Size effect on Adhesion force and validation

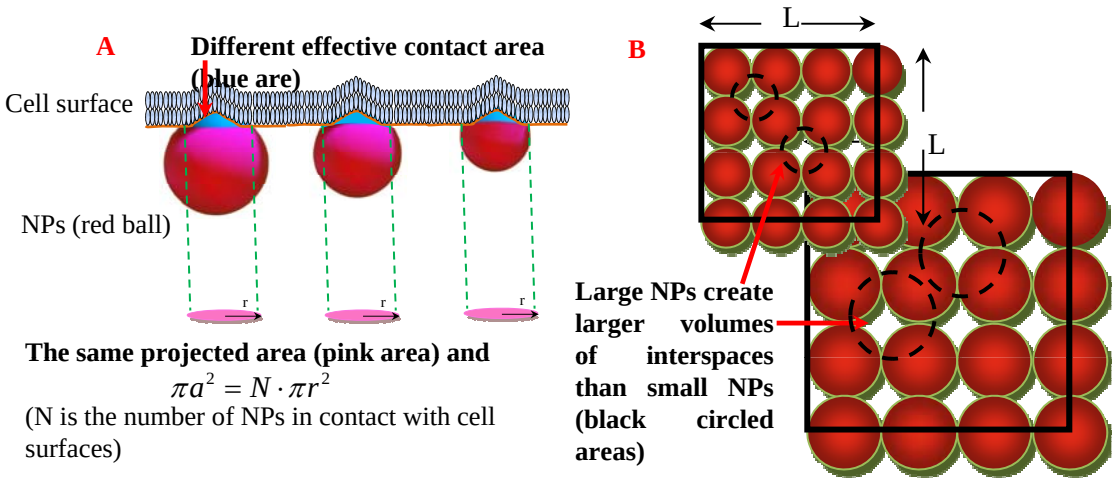

Schematics of modeling the size effect of NPs on adhesion force.

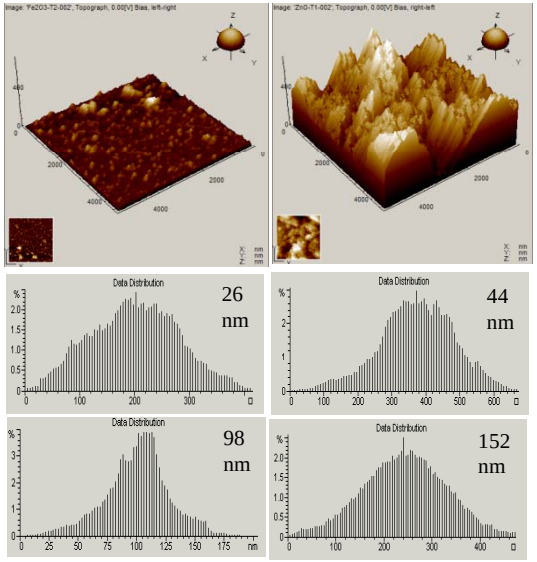

Surface topography and surface height distribution

Brief introduction to our proposed model of effective contact area used for explaining the size effect on adhesion force:

$$F_{ad} \propto \int_0^{R-\sqrt{R^2-r^2}} 2\pi\sqrt{R^2-(\sqrt{R^2-r^2}+x)^2}\,dx$$

$V=N\times[(2R)^3-(4\pi R^3/3)]/2 = L\times(4-2\pi/3)R^2$

$F_{ad} \propto 1/V$

$$F_{ad} = K\int_0^{R-\sqrt{R^2-r^2}} \frac{\sqrt{R^2-(\sqrt{R^2-r^2}+x)^2}}{R^2}\,dx \approx \frac{K(R-\sqrt{R^2-r^2})r}{R^2} \Rightarrow F_{ad} \propto \frac{Kr}{R}$$

Validations were made between *E. coli* cells and Al_2O_3 NPs, and between Caco-2 cells (human intestinal cells) and hematite NPs. For detailed information, refer to our manuscript.

Results and discussion:
1.3 Hydrogen bond estimation with force-distance curve and its support of our model of size effect

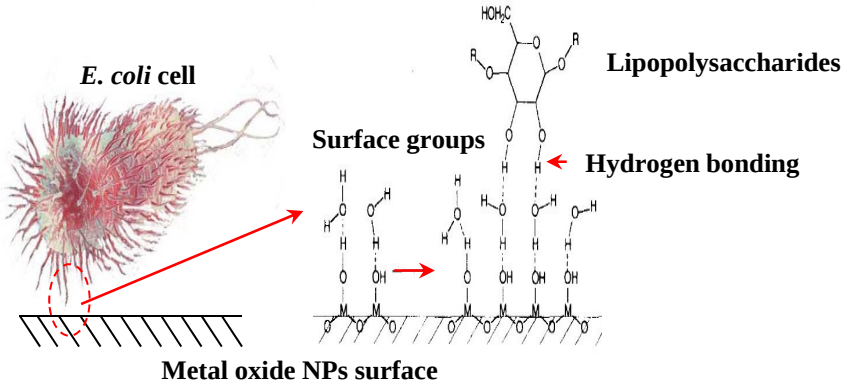

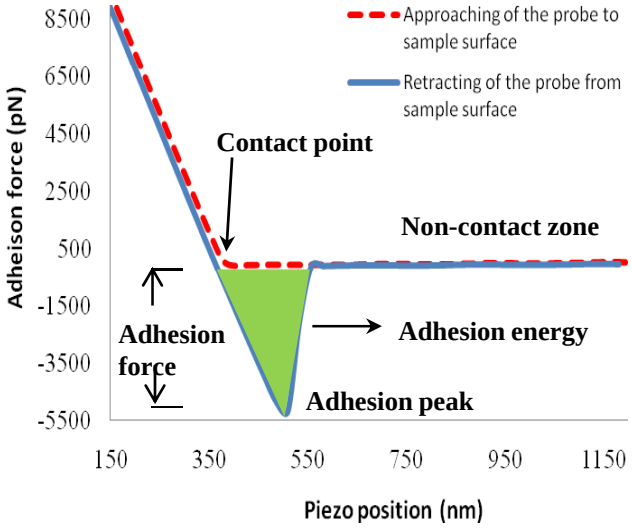

Adhesion energy and hydrogen bond calculation

Adhesion energy and hydrogen bond number

	NP diameter (nm)	Adhesion energy (J)	Hydrogen bond number on contact site area
Hematite NPs	23	$(8.5\pm1.7)\times10^{-16}$	$(8.5\pm1.7)\times10^{4}$
	42	$(7.7\pm2.2)\times10^{-16}$	$(7.7\pm2.2)\times10^{4}$
	53	$(1.0\pm2.6)\times10^{-16}$	$(1.0\pm2.6)\times10^{4}$
	98	$(3.7\pm2.0)\times10^{-17}$	$(3.7\pm2.0)\times10^{3}$
	150	$(3.6\pm1.2)\times10^{-17}$	$(3.6\pm1.2)\times10^{3}$
Al_2O_3 NPs	25*	$(6.5\pm1.7)\times10^{-16}$	$(6.5\pm1.7)\times10^{4}$
	30-40*	$(3.2\pm1.7)\times10^{-16}$	$(3.2\pm1.7)\times10^{4}$
	40-80*	$(1.2\pm1.7)\times10^{-16}$	$(1.2\pm1.7)\times10^{4}$
	100-120*	$(7.3\pm1.7)\times10^{-17}$	$(7.3\pm1.7)\times10^{3}$

The surface of an *E. coli* cell (average cell surface area is 6×10^{-12} m^2) contains about 3.5×10^{6} LPS molecules that can form hydrogen bonds with a mineral oxide surface. The contact site area between hematite NP array and E. coli cells is about 6359 nm^2 ($=\pi\cdot45^2$, estimated by JKR model). Thus, the average number of hydrogen bonds formed is 3709 ($=6359\times10^{-18}$ $m^2\times3.5\times10^{6}/6\times10^{-12}$ m^2).

Implications: NP arrays of small NPs may have a much higher contact area than large NPs.

Results and discussion:
1.4 Other mechanisms involved in adhesion that may explain the size effect

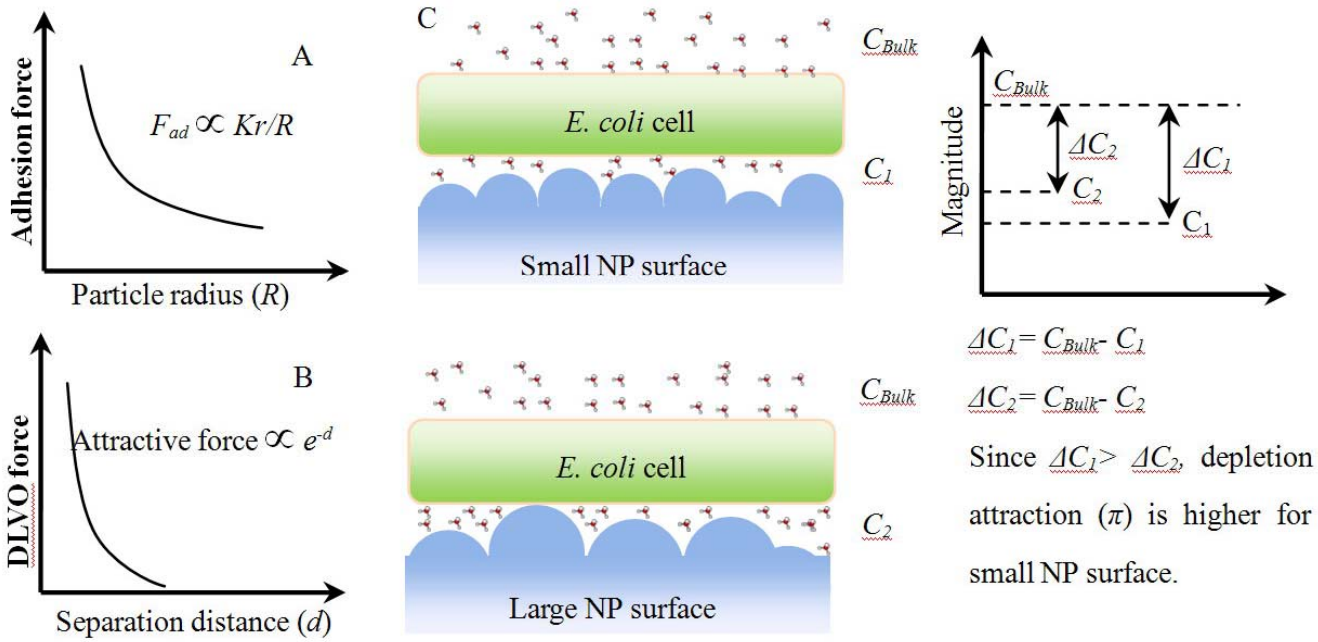

Representation of potential mechanism of size effect on adhesion force. A. Relationship between adhesion force (F_{ad}) and particle radius (R). B. Exponential decay of DLVO forces with distance. C. Depletion attraction (potentially different for cell surface interacting with different sizes of NPs.

Implication: a combined effect of three potential mechanisms were proposed to account for the size effect on adhesion force between NPs and cell surfaces, including the effective contact area, topographical effects on interfacial energy, and depletion attraction.

Results and discussion:
1.5 Correlation between adhesion force and adsorption rate of NPs toward cell surfaces

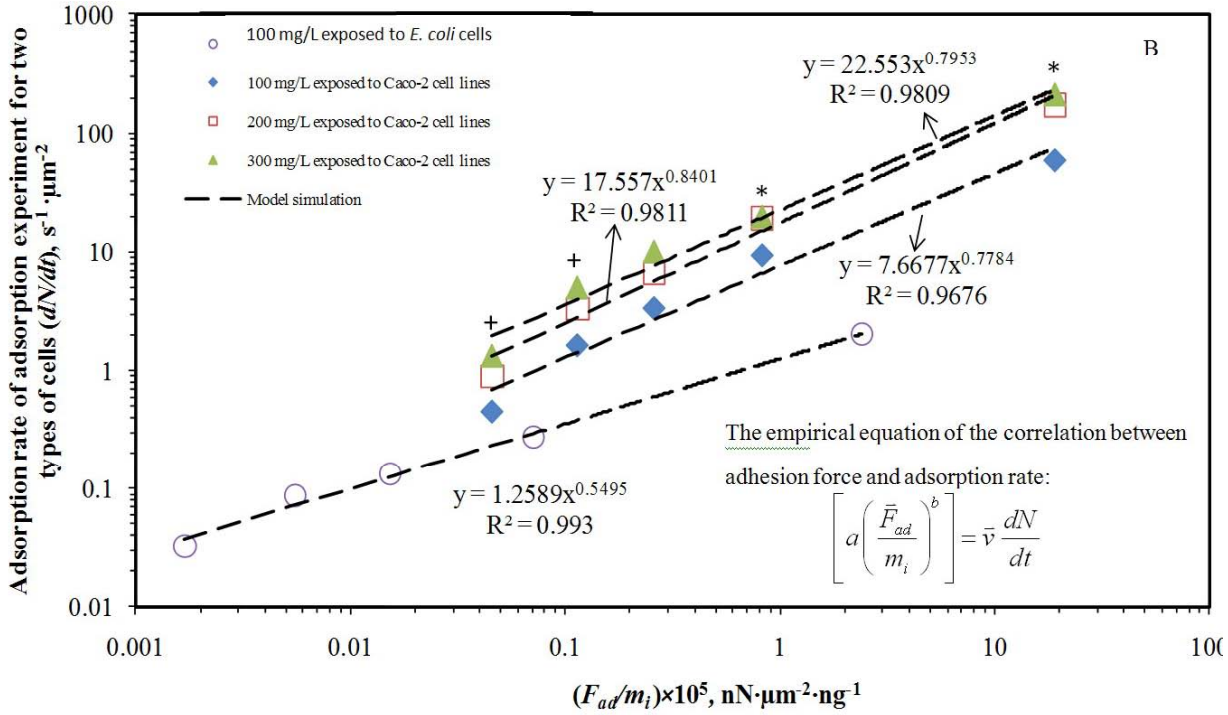

Comparison of the model simulation (dotted line) and experimental data. Symbols (* and +) indicate a significant difference (p<0.05) between the groups of three points marked by (+) and those groups marked by (*).

Significance: an important interconnection between adhesion force and adsorption rate of NPs onto the cell surface was established and the theoretical relationship can be derived mathematically from the conceptual model in the next slide.

Results and discussion:
1.5 Correlation between adhesion force and adsorption rate of NPs toward cell surfaces

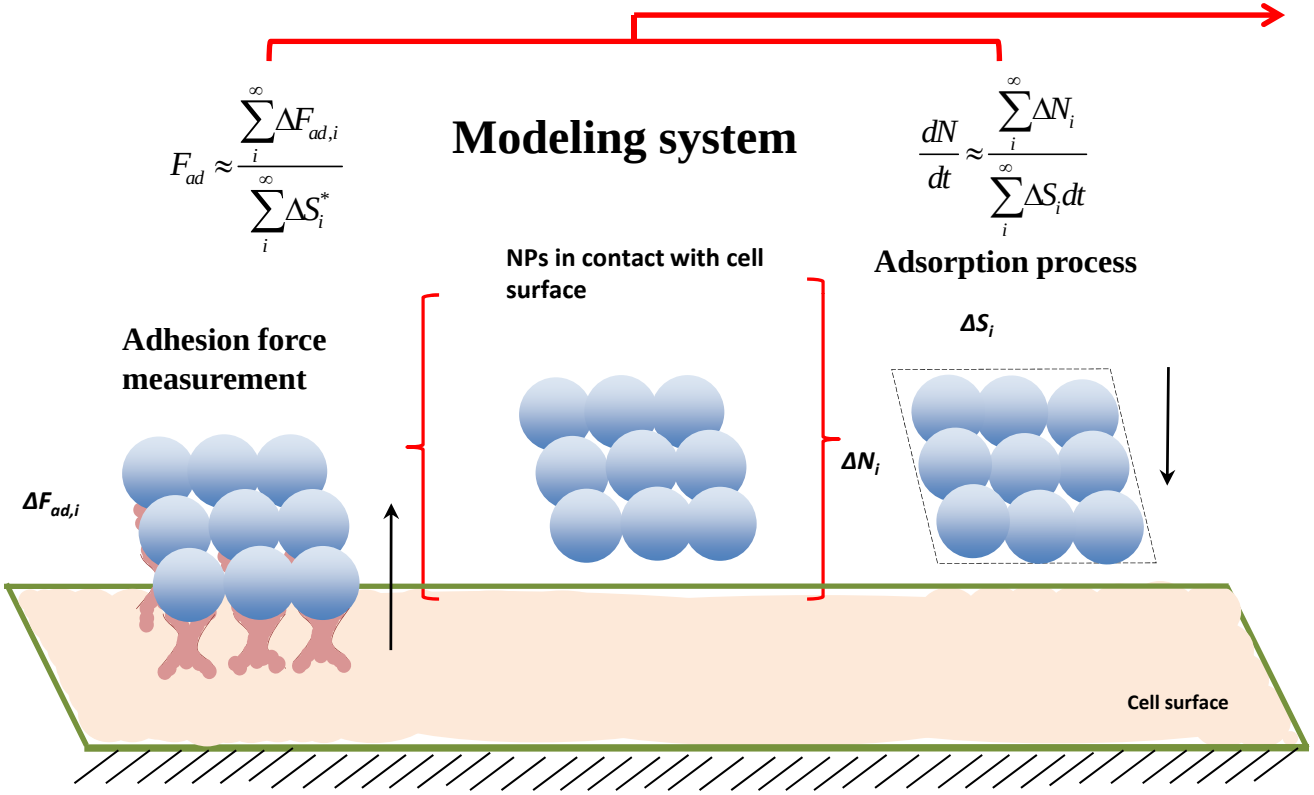

$$\vec{F}_{impact}\Delta t = \Delta(m\vec{v})$$

$$\vec{F}_{impact} \approx a\left(\vec{F}_{ad}\right)^b$$

$$\left[a\left(\vec{F}_{ad}\right)^b\right]dt = \vec{v}dm = m_i\vec{v}dN$$

Theoretical relation:

$$\left[a\left(\vec{F}_{ad}\right)^b\right] = m_i\vec{v}\frac{dN}{dt}$$

Modified equation:

$$\left[a\left(\frac{\vec{F}_{ad}}{m_i}\right)^b\right] = \vec{v}\frac{dN}{dt}$$

Conceptual model of the relation between adhesion force and adsorption rate (dN/dt).

This model was derived based on the impulse-momentum theorem and the relationship between the impact force and the resulted adhesion force. The above theoretical relationship between adhesion force and adsorption rate has the following parameters: m_i is the mass of a single NP; v is the approach speed of the cantilever tip toward the cells; a and b is the fit parameters.

Method and materials: 2. Cytotoxicity of hematite NPs on Caco-2 cells: size effect

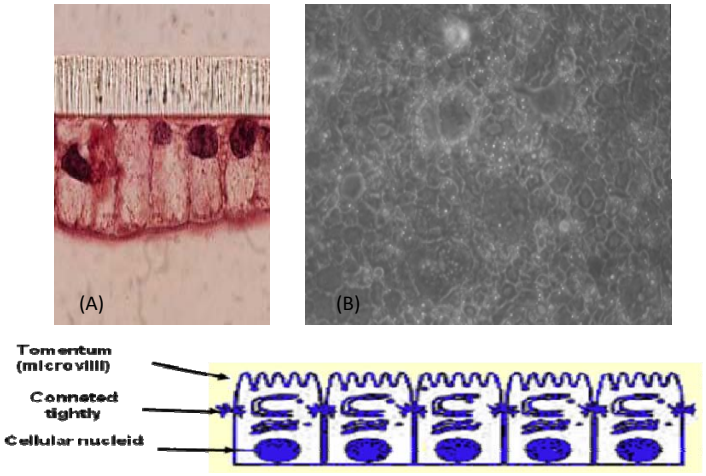

Figure 9 Microscopic images and structures of Caco-2 cells. (a): Side view of the cell lines; (b): phase contrast image for Caco-2 cell lines. The bottom drawing indicates the surface structure (microvilli) of the cell line.

Cytotoxicity was shown by junctional distruption of the cell lines and quantified with transepithelial electrical resistance (TEER). Cell penetration of NPs was visualized by confocal imaging.

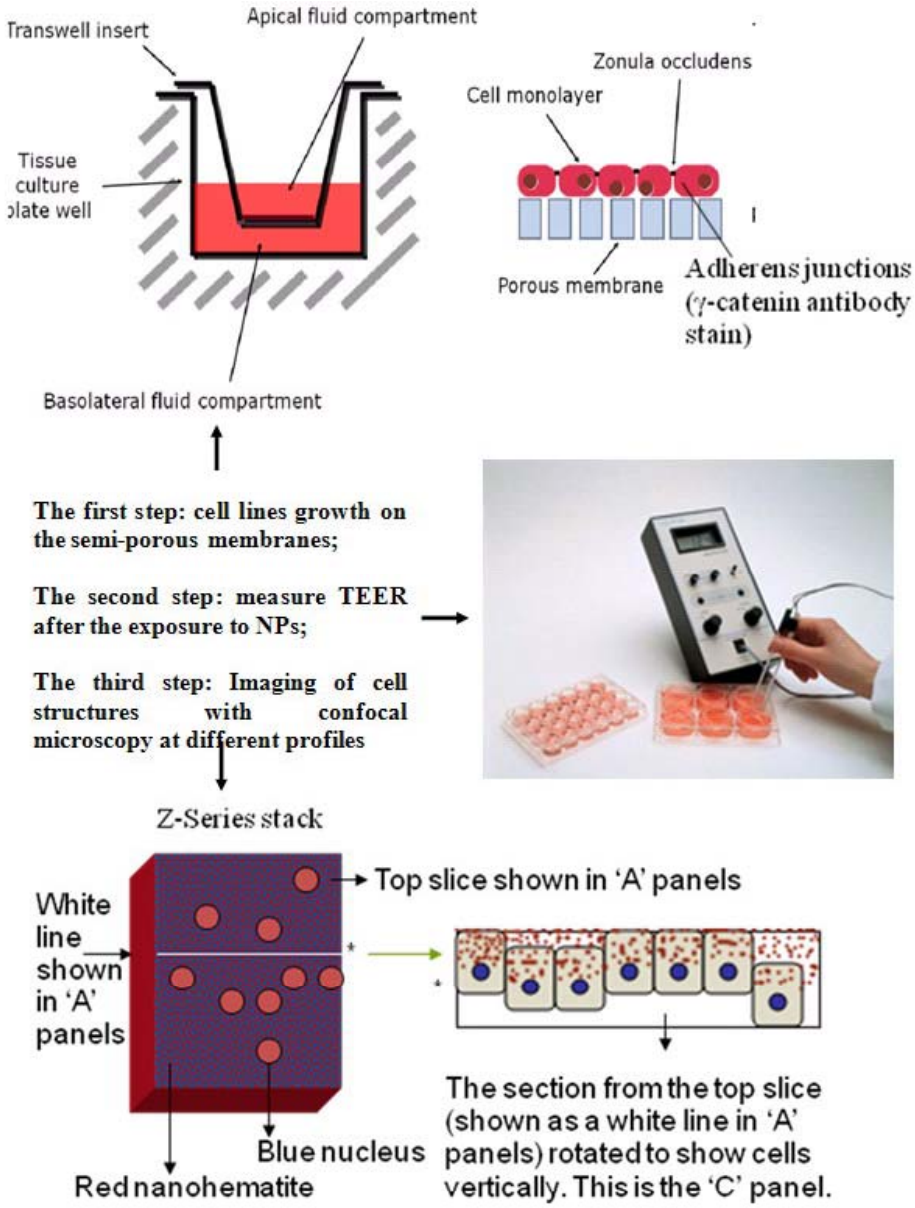

Figure 10 Schematics of cytotoxicity experiments with Caco-2 cells through TEER test and confocal microscopy

Results and discussion: TEER changes and junctional disruption induced by the exposure to NPs

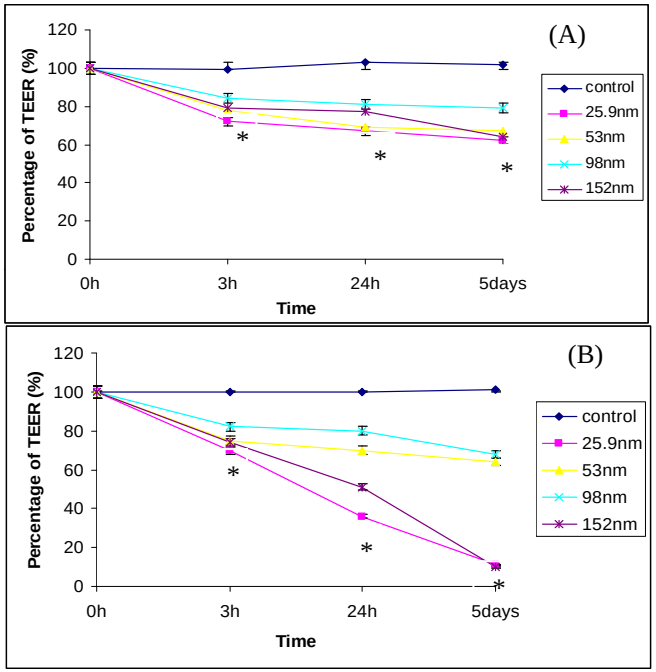

Figure 11 Caco-2 epithelial cells treated with 100 mg/L (A) and 300 mg/L (B) of various sizes of hematite NPs. Error bars represent mean ± SD (n=3), some of them may be obscured by the data marker; * = $p<0.002$ when compared to Control (Caco-2 cells without any added hematite NPs).

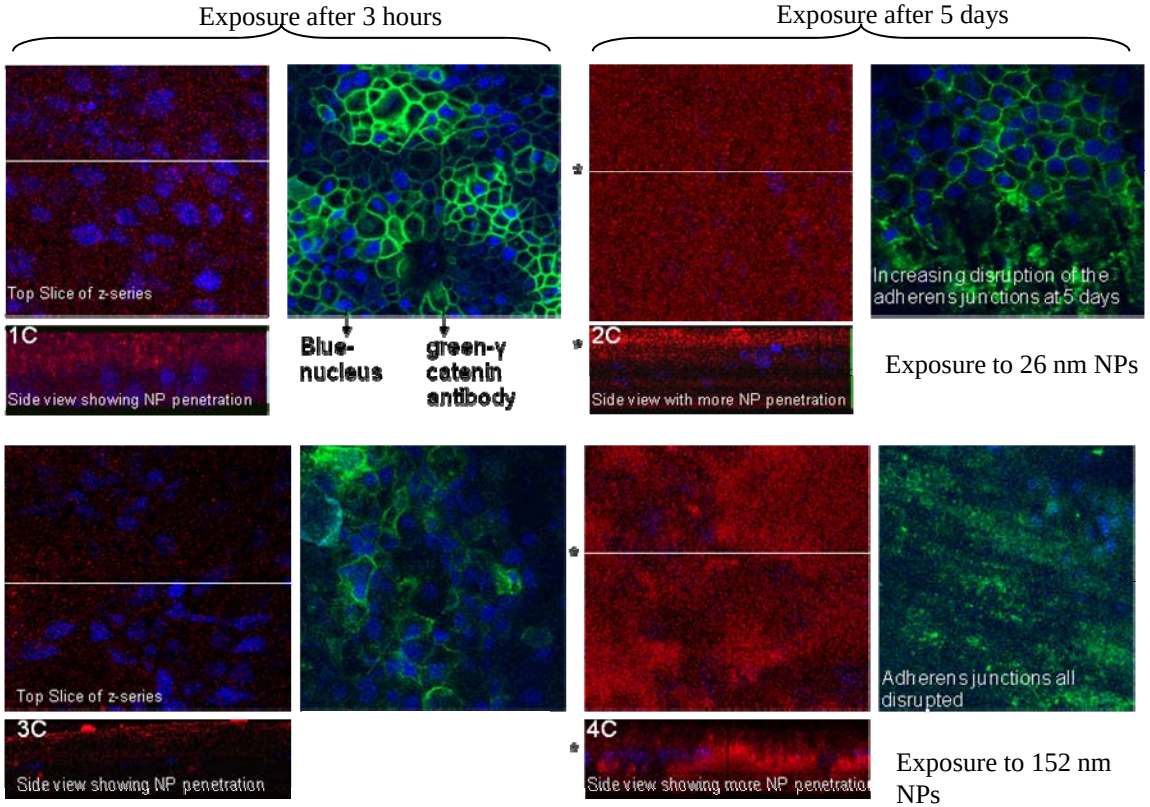

Figure 12 Representative confocal images of junctional changes of Caco-2 cells exposed to 26 nm and 152 nm hematite NPs. The important panels to consider are 3C and 4C. In these panels the red is the hematite NPs and blue color is the nucleus of a Caco-2 cell (refer to the picture of the cell in slide 2). The 3 panels show the penetration of NPs into cells at the specific time point and concentration tested. The nucleus for Caco-2 cells is toward the lower half of a cell, so NPs above the nucleus means NPs are inside the cell.

Future Plans

Next Year Plans

- Cell penetration of NPs and the governing factors
- Interactions between various NPs and representative human proteins such as biotinylated bovine serum albumin(biotin-BSA)
- The effects of environmental parameters (e.g., pH) on the interactions of NPs.

Long-Term Plans

- Build robust QSAR models based on fundamental data of adhesion force and its predicting impact on cells
- Provide information for manufacturing environmental benign NPs for industries.

Publications, Presentations, and Recognitions/Awards

1. **Wen Zhang, Madhavi Kalive, David G Capco, and Yongsheng Chen, Effect of Nanoparticle Size on Adsorption onto E. coli and Caco-2 Cells and the Role of Adhesion Force. Environmental Science and Technology, submitted.**
2. **Wen Zhang and Yongsheng Chen, Effect of Nanoparticle Size on Bacterial Cell Adhesion Force. being prepared.**
3. **Xiaoshan Zhu, Xuezhi Zhang, Wen Zhang, Yung Chang, Hu Qiang, and Yongsheng Chen. Potential Toxicity of Nanomaterials and their Removal. Proceedings of the Chicago International Environmental Nanotechnology Conference: Applications and Implications Oct. 7-9, 2008**
4. **Wen Zhang, Xiaoshan Zhu, Xuezhi Zhang, Yongsheng Chen. Potential Toxicity of Nanomaterials and their Removal (oral presentation). International Environmental Nanotechnology conference. Chicago, Michigan, October, 2008**
5. **Wen Zhang, Yongsheng Chen, et.al., Methodology Development for Adhesion Force Measurement between Nanomaterials and Cells Using AFM (oral presentation). 237th American Chemical Society National Meeting & Exposition, March 22 - 26, 2009 Salt Lake City, UT**